

High Gain Quasi-Yagi Planar Antenna Evaluation in Platform Material Environment for 60 GHz Wireless Applications

Arnaud L. Amadjikpè¹, Debabani Choudhury², George E. Ponchak³, and John Papapolymerou¹

¹ Georgia Institute of Technology, Atlanta, GA, 30332

² Intel Corporation, Hillsboro, OR, 97124

³ NASA Glenn Research Center, Cleveland, OH, 44135

Abstract — This paper presents the effect of platform materials on antennas designed for mobile platform integration at 60GHz. A four-element quasi-Yagi antenna array with small size is developed on liquid crystal polymer (LCP) material demonstrating 11.5 dBi peak gain in free space. An experimental study on the placement of the fabricated quasi-Yagi planar antenna array on laptop chassis material environments is performed in this work. The radiation characteristics of the antenna under test (AUT) are measured for different AUT positions in the laptop chassis material environment. Depending on the proximity of the platform material and AUT location, nulls may appear in the radiation patterns, the peak gain direction of the AUT shifts from the free space case by +30°, and the peak gain level decreases by about 2.5 dB in the worst case.

Index Terms — Planar arrays, endfire antennas, quasi-Yagi antenna, 60 GHz, antenna integration.

I. INTRODUCTION

With the increased need for high speed (over 1 Gbps up to 10 Gbps) wireless communication systems, the mm-wave band around 56-66 GHz has received a lot of attention during the last couple of years for the development of short-range, high data rate wireless links. The potential 60 GHz applications include point-to-point links, such as Wireless Personal Area Network (WPAN) and Wireless High Definition Multimedia Interface (HDMI). Due to the propagation characteristics at the 60GHz band, highly directive and high gain antennas are required at both the transmitter and the receiver to maximize the communication throughput.

To address the need for highly directional radiation patterns, endfire antennas such as the tapered slot antennas (TSA), endfire arrays and quasi-Yagi planar antennas can be considered. In [1], several TSA topologies have been designed in the mm-wave band. Although significant effort has been expended to reduce the size of the TSA, the overall length of the antenna is still about $4\lambda_0$. Large antennas are not appropriate for the 60 GHz mobile platforms which takes advantage of the small wavelength (5 mm in free space) to build on-chip antennas and maintain an overall small form factor. Recently, a 4×4 patch antenna array backed with an air cavity has been developed on low-temperature co-fired ceramic (LTCC) substrate [2]. The total size was less than $4\lambda_0 \times 4\lambda_0$, and the patch array exhibited good radiation performance. However, LTCC materials and the associated

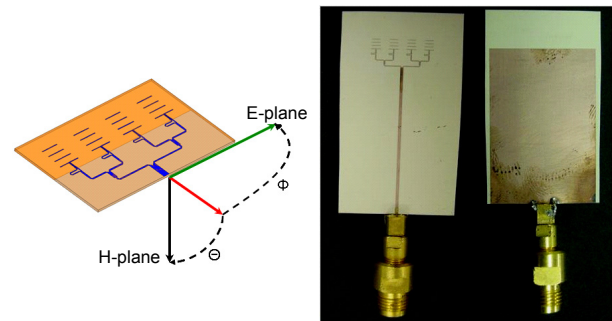


Fig. 1. 3D view (left) of the designed 4-element planar linear array (AUT) and photograph (right) of the top and bottom side of the fabricated AUT.

processing are typically more expensive than PCB-line materials and cannot conform to various surfaces.

For the aforementioned reasons, the quasi-Yagi planar antenna has been chosen as a good compromise, in terms of size and gain performance, between the patch and the TSA antennas [3]. The antenna in this paper is designed on Liquid Crystal Polymer (LCP) substrate, which is an organic, lightweight and flexible material with excellent loss characteristics up to 110 GHz, and very good mechanical stability [4]. The designed quasi-Yagi antenna is composed of a driver and three directors patterned on the top side of the substrate, and a pseudo-reflector patterned on the other side (Fig. 1). The three directors increase the directivity of the antenna, and to further increase the directivity, multiple quasi-Yagi antennas can be arranged together to form an antenna array. In this work, a 4-element linear array is designed and characterized in free space (Fig. 2). The 4-element linear array will be denoted as the antenna under test (AUT).

The purpose of this paper is to integrate the AUT on a laptop chassis, and then, characterize its behavior at different locations on the chassis. Up to now, the literature has primarily focused on the modeling and design aspects of 60 GHz antennas in free space [1], [2], and [5]. However, the design of a radiofrequency (RF) system at mm-wave would remain incomplete if the antenna operation is not evaluated when embedded in the casing of the host platform environment. In this paper, for the first time, experimental studies are performed to investigate the integration effects of a 60 GHz AUT on laptop computer materials.

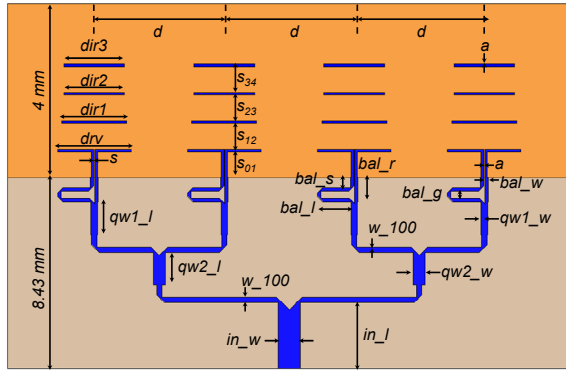


Fig. 2. Top view of the designed 4-element planar linear array (AUT) and description of geometrical parameters.

TABLE I
AUT DIMENSIONS (mm)

a	0.06	s_{01}	0.6	$qw1_w$	0.15
d	3	s_{12}	0.6	$qw2_w$	0.28
s	0.02	s_{23}	0.6	bal_s	0.25
$dir1$	1.5	s_{34}	0.6	bal_g	0.15
$dir2$	1.4	$qw1_l$	0.76	bal_l	0.775
$dir3$	1.4	$qw2_l$	0.76	bal_r	0.56
drv	1.7	w_{100}	0.125	bal_w	0.08
in_w	0.5	in_l	1.53		

This paper describes different scenarios where the AUT is positioned either on the screen display or on the base of the laptop under the chassis material. The different scenarios are compared to each other, and against free space performance.

II. QUASI-YAGI PLANAR ARRAY: DESIGN, SIMULATION, AND MEASUREMENT IN FREE SPACE

The topology of a single-element of the array is inspired from [3]. A driven dipole and three directors are patterned on the top side of an 8 mil thick LCP substrate ($\epsilon_r = 3.16$, $\tan\delta = 0.004$ at 60 GHz [4]). A truncated microstrip ground plane is patterned on the bottom side, and acts as a pseudo-reflector for the quasi-Yagi antenna. The driven dipole is fed with a coplanar strip (CPS) line which carries a TE_0 surface wave mode ($Z_{CPS} = 131 \Omega$). A 180° phase shift, introduced between the two balanced ports of a microstrip balun, ensures that only the coupled microstrip odd mode ($Z_{odd} = 86 \Omega$) is excited at the output of the balun (or input of the CPS line). With the geometrical parameters given in Table I, the impedance at the input of the balun of the single-element quasi-Yagi antenna is simulated to be 86Ω . Then, a microstrip quarter-wavelength transformer is connected to the unbalanced port of the balun. This transformation converts the input impedance of a single-element quasi-Yagi antenna to 100Ω .

Four identical single-element quasi-Yagi antennas are arranged in a linear array configuration, as shown in Fig. 2. A four-way power splitter/combiner is designed to equally distribute power to each single-element antenna. Simple T-

junctions are used to split power from a one-way to a two-way path. The power splitter/combiner lines are all designed to be 100Ω , such that the feeding network size is kept small. Then, it suffices to add two 70.7Ω quarter-wavelength transformers to up-convert the 50Ω signals coming from each two-element array into 100Ω signals. Finally, the two converted signals combine into a 50Ω signal, which flows into the 50Ω input microstrip line of the AUT. The microstrip lines are mitered at each bent corner to minimize the reflections created by these discontinuities. A center-to-center spacing d is defined between two single-element antennas. An optimization on the value of d has been performed with Ansoft's HFSS. It was found that by bringing the single-element antennas too close to each other ($d \leq 2.5\text{mm}$), the inter-coupling becomes too strong and the array gain decreases. If $d \geq 3.5\text{mm}$, side-lobe levels in the array E-plane become too high. Consequently, the optimum value $d = 3\text{mm}$ ($0.6\lambda_0$) was chosen to maximize the array gain and minimize the side-lobe level.

To verify the designed prototype, an AUT was fabricated and measured. The 50Ω input microstrip line is extended by 2.91 cm to minimize the reflections from the GPPO connector, which is connected to the AUT signal line with conductive silver epoxy. For the return loss measurement, a GPPO to 1.85 mm adapter is used to connect the antenna to the input port of a PNA. The measured bandwidth is 4.4 GHz (Fig. 3). The extra-resonances observed below 58 GHz and above 62 GHz are attributed to connector issues.

The radiation pattern and gain of the AUT have been measured at 60 GHz in a calibrated anechoic chamber. Two standard gain horn antennas were initially used to calibrate the system. A 1.85 mm to U-band waveguide adapter (0.8 dB loss) was required to connect the AUT to the measurement system. A 1.85 mm to 1.85 mm adapter (0.3 dB loss) was also used to match the polarities between the GPPO to 1.85 mm adapter, and the 1.85 mm to U-band waveguide adapter. The 2.91 cm extra-feed line also adds 1.46 dB loss, given that the simulated attenuation constant in a 50Ω microstrip line patterned on an 8 mil thick LCP substrate is 0.5 dB/cm. In all, the insertion loss that should be compensated from the measured data is about 2.56 dB. Once this compensation is done, the simulated and measured gains in the peak direction are 11.57 dBi and 11.47 dBi respectively. The measured peak

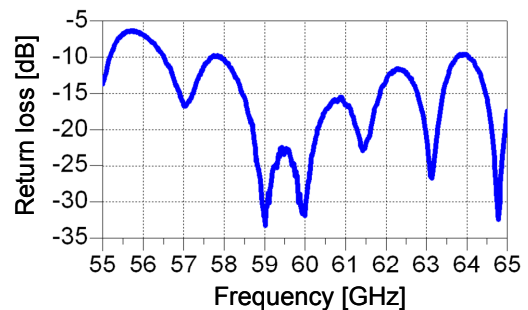


Fig. 3. Measured return loss of the AUT in free space.

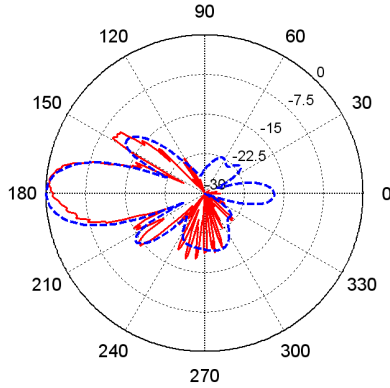


Fig. 4a. Simulated (blue) and measured (red) normalized E-plane radiation pattern of the AUT in free space.

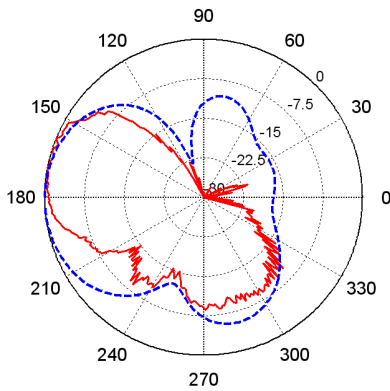


Fig. 4b. Simulated (blue) and measured (red) normalized H-plane radiation pattern of the AUT in free space.

gain was found by first, scanning the H-plane; and then the E-plane cut is taken in the direction of the previously found peak. The E-plane pattern is slightly asymmetric because of the balun configuration (Fig. 4a). The measured front-to-back ratio (F/B) is higher than 25dB. The measured H-plane pattern is narrower than the simulated one, but the shapes still match (Fig. 4b).

III. ANTENNA PERFORMANCE IN A PLATFORM ENVIRONMENT

A. Laptop modeling and description of the different scenarios

The laptop chassis model is shown in Fig. 5. The screen display is made of a dielectric laptop cover without the LCD and other circuit parts, whereas the laptop base is also made of a plastic laptop cover and includes metal at the base bottom.

Six different positions (P_1, P_2, \dots, P_6) are investigated in this work. P_1 and P_2 are very similar; the AUT is located at the top left and the top right corners of the screen display respectively. In P_3 , the AUT is located on the right edge of the screen display. P_4 is similar to P_1 except that the AUT is now positioned close to the laptop base. In P_5 , the AUT is located near the right edge of the laptop base, such that the AUT actually radiates perpendicularly to the screen display. Finally,

P_6 is the case where the AUT is positioned on the back side of the laptop base. Note that the AUT is placed outside the laptop base in P_6 .

B. AUT measurements in laptop environment

Conventional laptops chassis made with plastic materials are used in this study. The AUT substrate does not touch the laptop chassis, because the GPPO connector has an extra 1.42mm length from the center pin to its bottom edge. Hence, all these measurements are done with the actual antenna at $h = 0.28\lambda_0$ above the laptop chassis surface.

Figures 6a and 6b reveal that in $P_1, P_4,$ and P_5 , several nulls appear in the H-plane pattern. More precisely, in P_1 , a null appears around $+165^\circ$, which is actually the center of the beam in free space. Two factors could be at the origin of this phenomenon. First, the elevation of the antenna above the laptop chassis creates a reflected image from the chassis, such that the main field interferes with the reflected one, hence creating constructive or destructive interferences in specific directions. Second, as the AUT is located 1 cm away from the edge of the laptop chassis and facing 3 mm ($0.6\lambda_0$) high dielectric obstacles, diffraction might occur from the edge and the dielectric obstacles. Then, the diffracted fields might add or cancel each other, thus generating nulls or peaks in specific directions. The same analysis could be used to explain the observed nulls in P_4 and P_5 . Specifically, in P_5 , edge diffraction occurs at the junction between the screen display and the laptop base. The gain measured for $P_1, P_4,$ and P_5 is 9.82 (at $+148^\circ$), 11.02 (at $+150^\circ$), and 9.04 (at $+170^\circ$) dBi respectively. The peak gain is higher in P_4 than the two others because the portion of energy radiated between $+250^\circ$ and $+320^\circ$ (exactly in the proximity of the laptop base) is actually reflected by the laptop base, and redistributed toward other directions: this is a translation of energy conservation. Otherwise, the peak gain in P_1 , and P_5 is about 1.65 dB less than the peak gain in free space, which is in part due to the attenuation through the dielectric laptop cover. A separate measurement of the antenna radiating in a normal incidence with respect to the dielectric cover was performed to confirm that about 1.63 dB is absorbed by the lossy dielectric cover.

P_2 is similar to P_1 and P_4 , but it appears in Fig. 6a that the nulls in the pattern are less important, and the peak gain is 11.52 dBi at $+163^\circ$. The nulls are less important, probably because the 3 mm high obstacles are not present in P_2 .

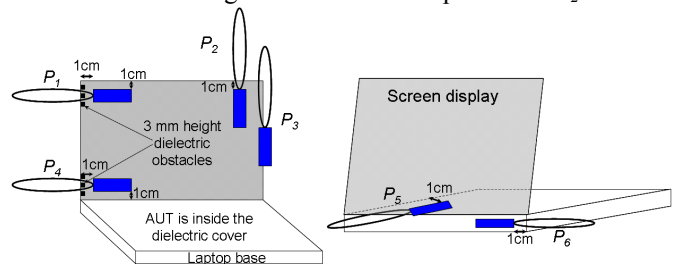


Fig. 5. Locations of the AUT on the screen display (left) and the laptop base (right).

In P_3 , the AUT is located right on the edge of the dielectric cover. Figure 6a shows that the H-plane pattern is relatively smooth, but the gain between $+135^\circ$ and $+175^\circ$ is attenuated by about 8 dB versus the free space. The peak gain is 10.13 dBi in the $+195^\circ$ direction.

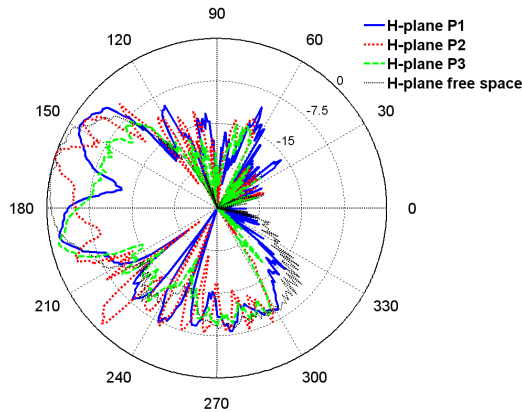


Fig. 6a. Comparison of measured normalized H-plane patterns for locations P_1 , P_2 , P_3 , and free space.

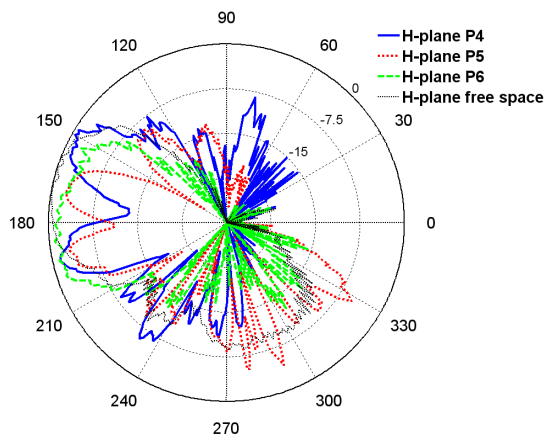


Fig. 6b. Comparison of measured normalized H-plane patterns for locations P_4 , P_5 , P_6 , and free space.

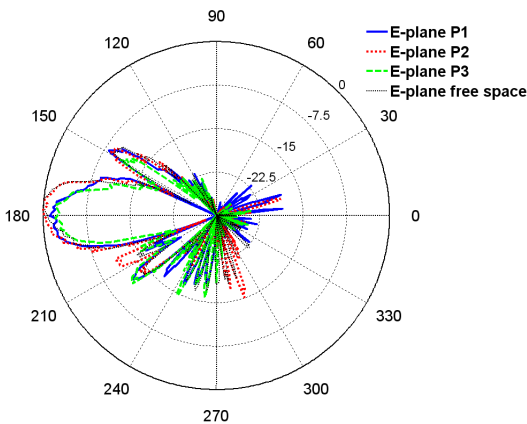


Fig. 7a. Comparison of measured normalized E-plane patterns for locations P_1 , P_2 , P_3 , and free space.

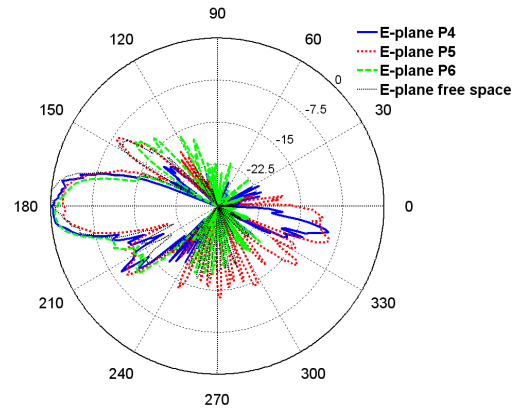


Fig. 7b. Comparison of measured normalized E-plane patterns for locations P_4 , P_5 , P_6 , and free space.

IV. CONCLUSIONS

The paper presents the design and measurement of an endfire antenna array on LCP material with relatively small form-factor and peak gain of around 11.5 dBi at 60GHz. The high gain 60 GHz planar linear array has been integrated, for the first time, in a laptop chassis environment. The level of the peak gain at 60GHz decreases when placed behind the laptop chassis materials because of the attenuation through the plastic laptop cover. Initial studies indicated that the peak gain direction depends on the antenna location and its proximity to the chassis material. In some cases, the peak gain direction shifted from the free space one. When the antenna faces critical diffracting obstacles, nulls appear in the pattern.

The observations in the presented paper are based on one type of laptop plastic chassis material. It represents a case of platform environment impact on 60GHz antennas. The particular antenna performance will also vary depending on the platform material type, chassis thicknesses, structures, environment, etc. It is recommended that 60GHz wireless antenna designs need to take the host platform materials and environment into consideration.

REFERENCES

- [1] S. Sugawara, Y. Maita, K. Adachi, K. Mori, K. Mizuno, "A mm-wave tapered slot antenna with improved radiation pattern," *1998 IEEE MTT-S Int. Microwave Symp. Dig.*, vol. 2, pp. 533-536, 1998.
- [2] A. Lamminen, J. Saily, A.R. Vimpari, "60-GHz patch antennas and arrays on LTCC with embedded-cavity substrates," *IEEE Trans. Antennas and Propagation*, vol. 56, no 9, pp. 2865-2874, Sept. 2008.
- [3] P.R. Grajek, S. Bernhard, G.M. Rebeiz, "A 24-GHz high-gain Yagi-Uda antenna array," *IEEE Trans. Antennas and Propagation*, vol. 52, no 5, pp. 1257-1261, May 2004.
- [4] D. Thompson, O. Tantot, H. Jallageas, G.E. Ponchak, M. Tentzeris, J. Papapolymerou, "Characterization of liquid crystal polymer (LCP) material and transmission lines on LCP substrates from 30 to 110 GHz," *IEEE Trans. Microwave Theory & Tech.*, vol. 52, no 4, pp. 1343-1352, April 2004.
- [5] B. Pan, Y. Li, G. E. Ponchak, M. M Tentzeris, J. Papapolymerou, "A Low-loss Substrate-Independent Approach for 60 GHz Transceiver Front-end Integration using Micromachining Technologies", *IEEE Trans. Microwave Theory & Tech.*, vol. 56, no 12, pp. 2779-2788, December 2008.